Araştırma Makalesi / Research Article

An Improved Deep CNN For an Early and Accurate Skin Cancer Detection and Diagnosis System

Zafer Civelek[1] iD **,Mohammed Hani Shakir Kfashi[2]** iD

[1]*Çankırı Karatekin University, Department of Electrical and Electronic Engineering, Çankırı, TURKEY*
[2]*Al-amriya, 10011 Baghdad, IRAQ*

Abstract
Skin cancer is considered to be the most common and dangerous type of cancer. Information technology techniques are required to detect and diagnose skin cancer. Therefore, there is a need for an early and accurate skin cancer diagnosis and detection by employing an efficient deep learning technique. This research work proposes automatic diagnosis of skin cancer by employing Deep Convolution Neural Network (DCNN). The distinguishing feature of this research is it employs DCNN with 12 nested processing layers increasing the diagnosis and detection of skin cancer accuracy. Beside neural network, machine learning techniques of naïve Bayes and random forest are also utilized to detect skin cancer. This research work results concluded that the deep learning technique are more effective than machine learning in terms of skin cancer detection. By applying Naïve Bayesian on the proposed system accuracy of 96% were achieved, similarly for Random Forest method, an accuracy of 97% were achieved. The accuracy of 99.5% were achieved by applying Deep CNN network. The performance of proposed system has been compared with other research work and it is concluded that it shows the higher performance compared to all conventional systems.

Key Words
"Skin Cancer, Machine Learning, Deep learning and Detection, Diagnosis"

* *Corresponding Author*: *mohammedhani0088@gmail.com*

1. Introduction

Cancer is common terminology for a variety of diseases that affect the human body. Cancer is basically an abnormal cells growth that attacks adjoining cells and spreads to organs of the body the process is known as metastasizing. Metastasizing cause's death and cancer is second leading cause of deaths internationally, approximately 9.6 million people die or one in sixth death is caused by cancer (Bray et al., 2018).

Skin cancer is greatest common and hazardous form of cancer diagnosed in human in recent years. It is found in various forms like melanoma, squamous and basal out of which melanoma is unpredictable to diagnosis. The occurrence of non-melanoma, and melanoma skin cancers has expanded over the last decades. Nowadays 132,000 melanoma skin cancer and between 2 and 3 million non-melanoma skin globally occur every year. Rendering to the records of Skin Cancer Foundation Statistic (SCFS) one out of five Americans have skin cancer. The 19th most common cancer in men and woman are Melanoma. Approximately in 2018 there were 300,000 cases of skin cancer. The 5th common cancer is non-melanoma cancer which effect 1 million people both male and female worldwide (Nahata & Singh, 2020). Furthermore, detection and diagnosis cancer disease are the most challenge to the doctors because of its resemblance. Skin cancer can't be detected with naked eye as it appears like a small mole in initial stages (Kadampur & Al Riyaee, 2020).

Information technology IT plays a huge role in diagnosis of diseases. Information technology improvement offers advancement in health care in terms of diagnosis, management, and support of the diseases. The physicians also get aids in diagnostic process due to improved decision support systems incorporated with evidence base medicines (Krive et al., 2015).
Many well studies have been established in skin cancer detection and diagnosis by using information technology. Some of them applied the machine knowledge methods for example Naive Bayes, Random Forest, Agent technology and Neural Network (Mahesh, 2020). Whereas, the best results in skin cancer detection and diagnosis have been observed with Deep learning techniques such as probabilistic neural network (PNN), Artificial Neural Network (ANN), and Convolution Neural Network (CNN).(Salvi, Acharya, Molinari, & Meiburger, 2021).

The conventional method of image classification needs protruding structures representation feed to the training classifier. The features structures can be color, shape, texture, or color images, while in skin cancer scenario, extraction of features and categorizing them on image base is difficult job to be done. The researcher's consideration has been drawn to use the CNNs to extract the structure features. Recent research has shown that CNNs abstraction capacity of layers has the capacity to excerpt together little level and high-level features (Kadampur & Al Riyaee, 2020). However, it is concluded from researches that CNNs will give best result in detection and diagnosis of skin cancer.

A skin cancer early detection and diagnostic automatic system is proposed in this research study. The proposed system constitutes two subsystems, first is machine learning and second is deep learning, the second one is the contribution of this research work. This work is segmented into seven sections, starting with the introduction. In section 2, the most effective and related previous work have been discussed. Whereas, the architecture of the proposed system is illustrated in section 4. Furthermore, section 5 presents the implementation and results of the proposed system. The analysis and discussion of the work is demonstrated in section 6. Lastly, section seven concludes the work.

2. Related Work

Numerous research studies have been established to detect and diagnosis, in this section, the most effective and related to our work were presented and discussed in detail. In the prior work of Daghrir et al. (Daghrir, Tlig, Bouchouicha, & Sayadi, 2020), melanoma skin cancer hybrid method has been introduced to analyses doubtful lesion. The proposed system depends on three methods for prediction purpose which are CNN and two machine classifiers. The machine learning classifier are trained based on color, borders and texture of skin lesion. Then, these approaches are joint to recover their presentations usage majority voting. The evaluation of functioning of the proposed system, the International Skin Imaging Collaboration (ISIC) dataset has been used and contains 640 images. According to the obtained results, the highest accuracy level of 88.4% is achieved using these three methods altogether.
Ulzii et al. (Dorj, Lee, Choi, & Lee, 2018), studied that the rapid and intelligent classification system for skin cancer is CNN. Also, the emphasize on the skin cancer classification using error-correcting output coding (ECOC), support vector machine (SVM). Evaluation of performance was done color RGB color mode (red, green, blue) format images of the skin cancers are collected from KAGGLE is used to test. Specific collection of images has noise in term of other organs and tools. The better results are obtained by cropping these images. Total of 3753 images were tested on proposed algorithms containing four types of skin cancers. The implementation results shows that the maximum average accuracy values are 95.1%.

Zhang et al. (L. Zhang, Gao, Zhang, & Badami, 2019), uses CNN classifier optimized with a meta-heuristic for trained network models to visualize dataset for skin cancer classification. Optimization of the neural networks are done through different steps; a little literature is available for deep learning base neural networks and its requests. In current study a novel method of monster optimization procedure is used for CNN model weight and biases optimization. The proposed technique comparison has been performed with ten general classifiers on two dataset of skin cancer counting Demurest Database and Dermi S Digital Database. An accuracy of 91 % is achieved while utilizing this method in comparison with conventional algorithms.

Kumar et al. (Kumar, Alshehri, AlGhamdi, Sharma, & Deep, 2020). proposed an upgraded tactic to notice three types of skin cancers in the initial stages. By using the proposed method, the input in skin cancer lesion, the classifier would distinguish between cancerous and non-cancerous type skin. The homogenous image region is separated by utilizing fuzzy C means in image segmentation. Different types of filters are used for preprocessing enhancing the attributes to images, while other features assessed by locale binary pattern (LBP), gray-level co-occurrence matrix (GLCM) and RGB color space. The false neural network is trained on difference development algorithms for further classification. Accuracy estimation are achieved for various features of skin cancer data set namely PH2 and HAM10000. The results from simulation result reals that the proposed method detect skin cancer effectively with a precision of 97.4%.

In former work of Boman and Volminger, (Boman & Volminger, 2018). attempts to implement the technique providing in the Stanford report and assess the performance of the CNN during the classification of skin lesion comparisons not tested in their research. Melanoma vs. solar lentigo and melanoma versus seborrheic keratosis are two previously unknown binary classification use cases. Inception v3 was trained for diverse skin lesions using transfer learning. A total of 16 training classes were used to prepare the CNN. During the CNN's validation, a 3-way classification attained an accuracy of 68.3 percent. With the same comparisons as the Stanford study, melanoma against nevus had a 71 percent accuracy rate, while seborrheic keratosis versus basal and squamous cell carcinoma had a 91 percent accuracy rate. For seborrheic keratosis vs melanoma, the accuracy rate was 84 percent, and for solar lentigo versus melanoma, it was 83 percent. Andre et al. (Pacheco, Ali, & Trappenberg, 2019). have developed a system that uses photos and meta-data to detect and diagnose skin cancer. The suggested system's performance was tested and evaluated using the ISIC 2019 dataset. Moreover, there are nine lessons in the dataset, yet, one of them is an outlier and is not current on it. To address the problem, we employ an collaborative of classifiers that includes 13 convolutional neural networks (CNNs), two ways for dealing with outliers, and a simple method for using meta-data with images. The findings achieved are consistent with the prior challenges, and the methods for detecting the outlier class and dealing with meta-data appear to be effective. The proposed system achieves an excellent result with an correctness of 91%.

3. Research Methods and Materials

In this section, the research and methods which have been used in this work are summarized as follows:

3.1 Testing dataset

The International Skin Imaging Collaboration (ISIC) was utilized to test and assess the proposed system's performance. It's a collaboration between academics and business aimed at making it easier to use digital pores and skin imaging to help lessen melanoma mortality. Melanoma is easily treatable when detected and preserved in its early phases (Daghrir et al., 2020),(Boman & Volminger, 2018). Through tele-dermatology, clinical decision support, and automated diagnosis, digital photographs of skin lesions may be utilized to instruct experts and general public about melanoma detection and also directly help in melanoma diagnosis. SIC works to achieve its goals through the development and promotion of standards for digital skin imaging and by engaging the dermatology and computer science communities toward improved diagnostics (Pacheco et al., 2019). ISIC is developing proposed standards to enhance the quality, privacy, and interoperability (that is capability to circulate images among clinical platforms and technologies) of digital skin images. Moreover, figure. 1shows a example of Melanoma and Benign cells.
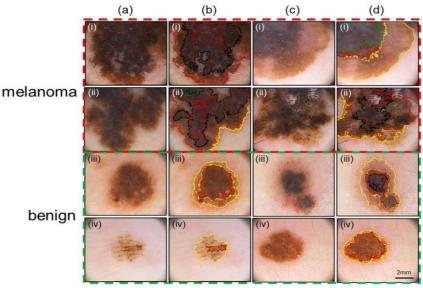

Figure. 1. Sample of Melanoma and Benign cells in different cases

3.2 Preprocessing stage

Preprocessing is an important stage and its first stage in the classification system that was used before the application of any type of classification technique. The dataset is containing a number of images, these images may obtain noise, shadow, and unimportant detail. This may result in misguiding results. Therefore, preprocessing main goal is to detect Region of Interest ROI and eliminate noise. Several techniques have been employed to do the functionality of preprocessing stage, the preprocessing techniques which have been used in this work are summarized as the following:

3.2.1 Fastest gaussian blur

The goal of employing the quickest Gaussian blur filter is to reduce noise from the contribution photos so that a Gaussian function can blur the image. When blurring a picture, the color shift from one facet of an image's edge to the other will be smooth somewhat than abrupt (Ku, Harakeh, & Waslander, 2018). The result is that fast fluctuations in pixel intensity are averaged out (Brekhna, Mahmood, Zhou, & Zhang, 2017). It is a convolution operation between Gaussian filter kernel and input images, Gaussian Blur can be calculated as in Eq. 1,

$$f * g[n] = \sum_{m=-\infty}^{\infty} f[m].g[n-m] \tag{1}$$

and,

$$f(x.y) = A.e^{1\left(\frac{(x-x_0)^2}{2\sigma x^2} + \frac{(y-y_0)^2}{2\sigma y^2}\right)} \tag{2}$$

3.2.2 YCbCr color space

After applying the quickest Gaussian blur output to the dataset's RGB color image, transform the image's color space from RGB to YCbCr in this stage to make the ROI (diseases region) more evident in infected and healthy images (Ku et al., 2018),(Yang, Zou, Zhou, & Shi, 2020). The luminance and chrominance in a picture are separated of YCbCr color space. The image's brightness is saved in the Y-channel. Cr and Cb channels store in red and blue direction chrominance values accordingly.

3.2.3 Fast fourier transform (FFT)

The application channel for image space is far faster than for images in iteration areas (Grigoryan & Agaian, 2020), to convert copy from spatial copy space to repetition part and FFT technique is employed. This stage seeks to improve and make more features of the image visible in a shorter amount of time, therefore the images inverse and forward transformation they will be required in frequency domain to apply FFT technique to the YCbCr images.

3.3 Classification stage

- *Naive bayes*

The most frequent classification algorithms are naive Bayes approaches, which are based on Bayesian probability theory (Mahesh, 2020),(Pranckevičius & Marcinkevičius, 2017). The number got by dividing the number of instances A by the entire number of proceedings is the likelihood of an event A. it is well know that probability value lies between 0 and 1 it is represented in percent here. For instance, the probability of picking a letter C, D, E, F, G, or H at chance is p (sound) = 1/6, or roughly 16.67 percent. Because they have no influence on one other, the probability principle has two independent events.

$$P (B \mid A) = p (A). (B)/ P (A) \tag{3}$$

Thomas Bayes' understanding of the Bayesian technique was a major influence on the Bayesian notion. In 1763 after his demise, his idea was printed in the Philosophical Transactions of the Royal Society of London in an article titled "On the Problem about the Opportunity" (Lewis, 1998). Bayesian statistics is apprehensive with calculating the likelihood of a specific pattern (sample) X assumed for a large number of comments. The probability of the posterior (i.e., the pattern of specific class probability I providing its pragmatic values) or the hypothesis of a class is determined in the following equations for pattern X.

$$h, P (h|X), \text{ is as indicated } P (h|X) = \frac{P(X|h)P(h)}{P(X)}, \tag{4}$$

Here P (h) value is associated from likelihood of h (such that N and |h| are pattern number in h class and total number accordingly, moreover assuming all theories equal probability). The provisional likelihood of term X is represented by P (X|h) depends on h; ant previous probability of X is P(X). Maximum Posterior Hypothesis MAP is utilized to denote the optimum P h $= (\frac{|h|}{N})$

$$P\frac{h}{X} \text{ h. class.} \tag{5}$$

$$h_{MAP} \equiv \arg \max_{h \in H} = \arg \max_{h \in H} P(X|h)P(h) \tag{6}$$

Set of assumptions is represented by H.

The efficiency of Bayesian classifier can be improved in term of least error rate due to likelihood of data probity. The predicted loss of a choice which is also known as conditional risk value is smallest in this case. This statistically optimal categorization criterion serves as an agreed-upon standard for the output comparison of various rating algorithms (Pranckevičius & Marcinkevičius, 2017).

That is a well-known probabilistic classifier that is utilized in a variety of requests. The Bayes classifier is founded on the Bayes theorem whereas naive adjective is generated by considering mutually independent characteristics of the data set. In other words, exercise instances features are supposed to be independent of one another in the class setting (Gedraite & Hadad, 2011). The NB classifier signifies all patterns X as an n-dimensional course representing features values of [a1, a2... and] assuming that it is c1, c2... Etc. When and only when class C I assigns an unknown pattern X, the classificatory expects it to drop to the class with the peak post-conditional probability, as shown in equation. 7, 8.

$$P(C_i|X) > P(C_j|X) \tag{7}$$

and,

$$P(C_i|X) = \frac{P(X|C_i)P(C_i)}{P(X)} \tag{8}$$

However, to minimize the required computing costs, the classifier marks the naïve or simplistic supposing that the attributes (with total number is given by n) are independent provisionally from all other. The independency of the class-conditional i can be demonstrated as follows:

$$P(X|C_i) = \prod_{j=1}^{n} P(f_j|C_i). \tag{9}$$

Because $P(X)$ represent each class constant value and $P(C_i) = \frac{|C_i|}{N}$, the NB classification must maximize just $P(X|C_i)$. Since it counts class distribution, this drastically reduces the cost of calculation. Bayesian classification is simple, using a unity data scan to offer a great level of precision (Pranckevičius & Marcinkevičius, 2017).

- *Random forest classifier*

The classifier random forest is false of a series of tree classifiers {h (x, θ_k) = 1, 2. where k is a distributed unequally scattering vector so all tree chooses a component for the shared category at the input x [20]. A tree selection is shaped by Random Forest Arbitration. To make each and every tree in a Random Forest technique, Breiman utilized the ensuing procedures: This is a bootstrap test; if N is prep set size, N files are provided precisely, but by dividing it from the original data. This demonstration will act as a warm-up for the tree's growth (Krive et al., 2015). If M input rudiments and the number M is set with the goalmouth of picking m rudiments in M at random at all location, with the finest allocation of these m components being to detach the midpoint. The assessment of m's circumstantial arena expansion is preserved (Speiser, Miller, Tooze, & Ip, 2019). Equation 10 may be used to calculate it.

$$RE^* = f_{xy}\big(mg(X.Y)\big) < 0 \tag{10}$$

Margin function can be signified as follows

$$mg(X.Y) = av_k I(h_k(x) = Y) - max_{j \neq Y} av_k(h_k(X) = j) \tag{11}$$

The margin function determines how far the average quantity of votes for the right magnificence exceeds the average vote for some other elegance at (X, Y) (Speiser et al., 2019). The Random Forest's strength is expressed in terms of the predicted value of the boundary purpose as,

$$S = E_{X.Y}\big(mg(X.Y)\big) \tag{12}$$

If ρ is the imply cost of the correlation between base trees, an top sure for generalization error is given by,

$$PE^* \leq P(1 - S^2) / S^2 \tag{13}$$

- *Convolutional neural networks (CNN)*

CNN is a sort of feed-forward false neural network that constitutes many convolutional layers preceded by one or additional completely linked layers, analogous to a typical multi-Layer perceptron (Mahesh, 2020). CNN is a feed-forward neural network, as seen in figure. 2. The indication is handled straight here, with no loops or cycles. This is signified as (N. Zhang et al., 2020):

$$G(x) = gn(gn - 1(\dots(g_1(x)))) \tag{14}$$

Here N signifies the hidden layers count, input signal is X, and gn represents the purpose conforming to layer N. A convolutional layer in a simple CNN model contains a purpose g with several convolutional kernels (h1, ... hk-1, hk). Each hk represents a linear purpose in the kth seed, as seen in (Munir, Elahi, Ayub, Frezza, & Rizzi, 2019):

$$h_k(x.y) = \sum_{s=-m}^{m} \sum_{t=-v}^{n} \sum_{v=-d}^{w} v_k(s.t.v)x(x-s.y-t.z-v) \tag{15}$$

where (x, y, z) is the pixel location of the input X, m is the tallness, n is the width, w is the filter depth, and v k is the weight of the kth kernel (Munir et al., 2019).
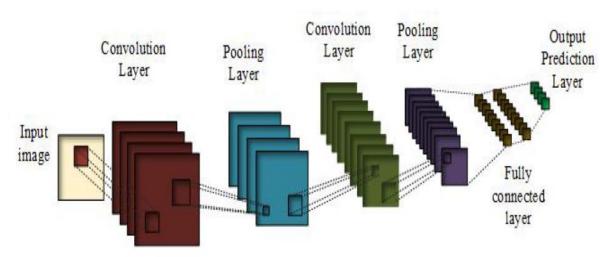

Figure. 2 The architecture of CNN

The primary reason for grouping in CNN is to benefit from down sampling, which enumerates surrounding pixels and substitutes it in display in a region of summary attributes. Pooling lowers dimensionality while maintaining the immutability of rotational, and interpretative modifications. One of the most well-known polar capacities (N. Zhang et al., 2020). is max pooling, wherever efficacy is the best approximation of area in pixel of rectangular order. The display undertakes the typical worth of the rectangle zone in normal grouping mode. Normal weighting is another type that is dependent on the right focus pixel routes. Grouping aids in making the depiction immutable for slight variations in information interpretation. In all circumstances, the following condition provides Atrous Convolution: Eqs. (Grigoryan & Agaian, 2020), (Pranckevičius & Marcinkevičius, 2017), (N. Zhang et al., 2020). provide the Atreus Convolution:

$$y[i] = \sum_{k=1}^{k} x[i + r.k]w[k] \tag{16}$$

here x[i] is one-dimensional contribution sign w[k] would be the k-length sieve, and r would be the input signal sampling stride rate. y[i] is the outcome of the Atrous difficulty. Atrous difficulty is done at each position I on the production y, and also a sieve w by the Atrous degree r, which correlates to the pace degree. Bottomless remaining learning is usage to solve the performance squalor, which occurs when bottomless networks collide, increasing depths, precision, and degradation saturate. Layers that are clearly layered can reside in residual map as an alternative of the required basic map. Experimental data reveals, residual network optimization is fairly simple, and precision may be attained with a substantial depth increment. In deep neural networks, good connections assist information to transcend (Speiser et al., 2019). Going through too many levels might result in the disappearance trend, which is a progressive loss of information. Escape connections offers benefit of lower-level information further lowering, creating minute features easier to identify. Over-polling activities have resulted in the loss of some local information, whereas escape connections allow extra information of final layer to be obtained in order to improve ranking accuracy (N. Zhang et al., 2020).

Numerous activation function can be used in the activation layer (Daghrir et al., 2020):
i.   Equation (17) gives sigmoid activation function (Gedraite & Hadad, 2011).

$$\sigma(x) = \frac{1}{1 + e^{-x}} \tag{17}$$

The above equation is nonlinear as a consequence the combination is nonlinear function allowing us to create layers. It has an x-axis range of -2 to 2 and a y-axis range of fairly vertical, signifying dramatic variations in the values of y in response to tiny variations in x values.
ii.   the activation function also has a property that its output remains in range of (0, and 1)

iii. Tanh function can be explained as (Rey-Barroso et al., 2021).

$$f(x) = \tanh(x) = \frac{2}{1 + e^{-2x}} - 1 \tag{18}$$

known as scaled sigmoid function

$$\tanh(x) = 2sigmoid(2x) - 1 \tag{19}$$

The range stretch between -1 to 1 and tanh has much stronger gradient than sigmoid purpose.
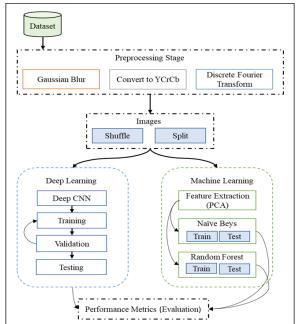
iv.   Rectified linear unit (ReLU) is popular employed activation function (Rey-Barroso et al., 2021), such that g indicates a nonlinear pixel-wise function. If x is positive, it returns x; else, it returns 0 (Wang, Zhang, & Wei, 2019).

$$g(x) = mx(0.x) \tag{20}$$

ReLU is intrinsically nonlinear as a result its multiple is nonlinear as well, allowing multiple levels to be layered together. It has a range of 0 to infinity, which means it can also explode up activation. G lowers the size of the characteristics for the polling layer, though the bottom liner performs conferring layer. 1 * 1 confessional kernel is present in the fully enclosed layer. A soft mix in the prediction layer forecasts the likelihood of Xj belonging to a distinct class (Pranckevičius & Marcinkevičius, 2017), (N. Zhang et al., 2020).

4. The Proposed System Architecture

In this work, an Automatic Skin Cancer detection and diagnosis System has been proposed; it is founded on deep learning by employing the Deep CNN and machine learning by employing the Naive Bayes, and Random Forest. The proposed system has the ability to detect and diagnose Skin cancer in early stage. figure. 3 displays the building of the proposed system; it is consisting of several main steps as following:

Figure. 3. The architecture of the proposed system.

ISIC is creating resources for the dermatology and computer science communities; Goals include a huge and growing open-source public access archive of skin pictures. This repository is a public picture resource for education, research, and the development and testing of diagnostic artificial intelligence systems. ISIC is engaging the stakeholder communities through meetings, publications, conferences, and the hosting of artificial intelligence Grand Challenges. In this work, the data contains 3297 images and two classes which are benign and malignant in different cases. The dataset is originally segmented in two training and testing. Furthermore, a total of 2637 images is used for exercise and a total of 660 imageries have been used for challenging and evaluation the performance of the proposed system.

The most critical stage in classification systems is preprocessing. This stage is divided into four major sub-stages, as indicated in figure. 4, and elucidates as follows:
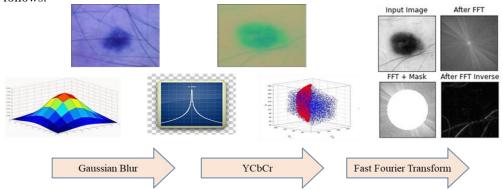

Figure. 4. The preprocessing Stage

Gaussian blur is a process of convolution among two input pictures and filter kernel. However, this phase demonstrates the information of the quickest Gaussian blur, since the algorithm's inputs are Skin cancer photos and the radius indicates "sigma" or "standard deviation." Also, this stage, 2D functions will be denoted as value matrices, and the weight is referred as kernel. The regular, i.e., the total of function quantity about I j], increased by a heaviness, is the value of convolution at I j]. figure 5 demonstrations of the output of the quickest Gaussian blur stage.
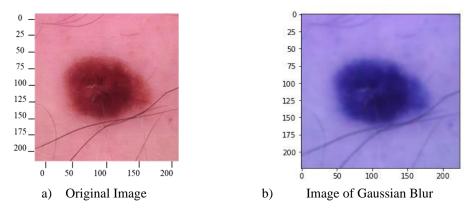

a)   Original Image   b)   Image of Gaussian Blur

Figure. 5. Fastest Gaussian blur algorithm output example

The green component has the biggest impact on the Y-channel, as seen in figure. 6, since natural eyes perceive green, next to red and blue sections. When R, G, and B are all in the variety of 0... 255, Y is also in the range of 0... 255, whereas Cb and Cr are in the range of - 128... 127. The number 128 is usually allocated to channels Cb and Cr to consider them component of an unregistered byte data kind.
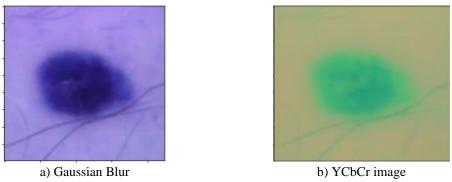

a) Gaussian Blur   b) YCbCr image

Figure. 6. An Example of convert color image from Gaussian to Ycbcr

The FFT procedures outlined in (6) are applied to the anthracnose picture shown in Figs. (6) The sign falloffs into broken sections to generate frequencies. The picture goes from space region to reproduction area after the FFT. Each point in the first figure refers to a certain repeat. When FFT is applied the picture is altered for DC section F (0, 0), represents illumination, is presented in image's midpoint. Furthermore, the white region in the intermission picture in Fig (3.6), exhibited afterward the FFT, demonstrates the extraordinary intensity of repetition. low frequency ranges are at the corner of images. Hence when two points are joined together, strong frequencies are gained at low frequencies at angle white region. common for greatest imageries. The FFT Cover 2-D FFT shown in figure. 7 can be interpreted and inverted, allowing it to be relocated devoid of behind data components. The zero-repetition portion is shifted to the area's midpoint, creating the picture more apparent to people. Furthermore, this analysis can assist us in running the High / Low Pass channel without issue. Finally, the opposite Fourier Transform was used in Fig. 7 to get the first picture deprived of little incidences.
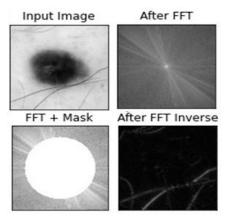

Figure. 7. Fast Fourier transform (FFT) steps

The morphological gray dilation operation is the final stage in preprocessing. The Gray image obtained in the previous step has strong and weak pixels, hence the motivation of this section is to improve the visibility of weak pixels, to fill in objects small holes, and eliminate small regions on the resulting image that are considered unimportant areas or noise, while keeping the useful areas for processing in the following steps. By adding pixels to the object bounds, an operation of dilation stretches the pixels of an copy and extends the limits of an thing. More specifically, the output pixel worth equals the greatest value of all the neighboring pixels. However, as the above discussion, the proposed system is segmented into two subsystems. One is system getting to know and second is deep mastering. Moreover, because the dataset is sorted by class there is a need for shuffling in the case of machine knowledge. Whereas, in the case of deep knowledge there is a need to riven the dataset to exercise and testing to evaluate the obtained results and then compare with the related work. The dataset is divided into two sections, the first of which contains 70% of the data used to train the proposed system. The second half, on the other hand, contains of 30%, which has been utilized for performance test of the suggested system. This segmentation was carried out in accordance with the relevant study, which they compared to our suggested model. To acquire the gray pictures in preprocessing phase, the dataset was scuffled and separated as shown underneath:

- *Shuffling dataset:* Python's "random. Shuffled" function was used to reorder the data collection. This is a request based on arbitrary number generation for computational restructuring The picture query, formerly in sequential sequence, is now intermingled entire database after application.
- *Splitting dataset:* Associated project portion is known as database; the 30 percent of the whole dataset is presented as test set and the residual data is displayed in same 70/30 form. The remaining funds are utilized to train the algorithm. Approval and preparation of sets are performed for developing algorithm, whereas test set is employed afterward classifier makes predictions.

5. Implementation And Results

There are several types of disease could affect the skin, the most common and dangers one is the cancer. Therefore, an early and accurate skin cancer Detection and diagnosis system is required. Subsequently, in this section, a set of experiments are conducted to test the hypothesis and determine if it is efficient to detect and diagnose the Skin cancer disease.

5.1 Implementation environment

- Implementation environment is explained which is separated into two parts: hardware and software implementation as shown below.
- Software: Python and Windows 10 were used in this study. Python also has a plethora of libraries, classes, and functions at its disposal. However, because it completely supported the planned system environment, this study primarily employed the Graphic User Interface (GUI) library to develop simulation. In addition, python supports standard image processing tasks like as picture display, simple manipulations such as cropping, rotating, flipping, and so on, copy division, and attributes removals, copy restoration, and copy recognition. Python is an excellent tool for copy dispensation workloads. Python is gaining admiration as a

technical programming linguistic, as well as the unrestricted accessibility of numerous cutting-edge copy dispensation gears in its bionetwork.

- Hardware: The imitation is run on a single laptop with an Intel (R) Core (TM) i7-5500U CPU running at 2.40GHz and 16 GB of RAM.

5.2 Performance of the proposed system

The performance of the proposed system is analyzed by dividing it into two subsystems, which utilize the different classification algorithms and follow same steps of preprocessing dataset. the first system shows skin cancer diagnosis through machine learning Random Forest, and naïve Bayesian algorithms. The second subsystem provides skin cancer illness analysis founded on deep knowledge utilizing a DCNN. Finally, based on accuracy measures, the acquired findings for both systems were compared to determine the optimal performance of each subsystem in diagnosing skin cancer illness. As a result, the outcomes of the proposed system each stage are depicted in the subsections below.

5.2.1 The results of preprocessing stage

The proposed system's initial stage is to import images from the ISIC dataset. Furthermore, as seen in the table, the dataset has two distinct classifications (1).

Table 1. Skin cancer Dataset Classes

#	Class	Label
1	Malignant	C1
2	Benign	C2

Furthermore, because the dataset is so large, five picture samples were chosen for each class. Figure 8 depicted the picture examples for all lesson along with their histograms. The histogram is crucial in this case to display the pixel distribution in the original picture so that the influence of the processes conducted on the images of every class can be determined by relating the outcomes of each operation to fundamental histogram In. Moreover, the sample of inputted images for two classes is shown in figure. 8, the Benign represents C1 and Malignant represents C2.
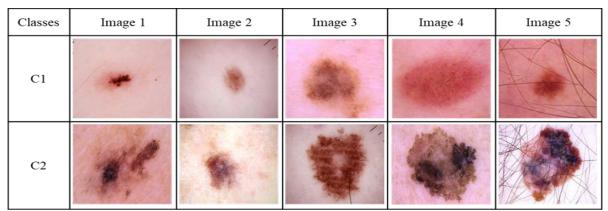

Figure. 8. Sample of Benign and Malignant Cells Images.

However, several steps have been done in the preprocessing stage to eradicate the noise and to notice the area of attention (ROI). Also, to make the image readable by the applied algorithms. Whereas, the output of preprocessing stage is illustrated in the bellow figure. 9a and 9b.
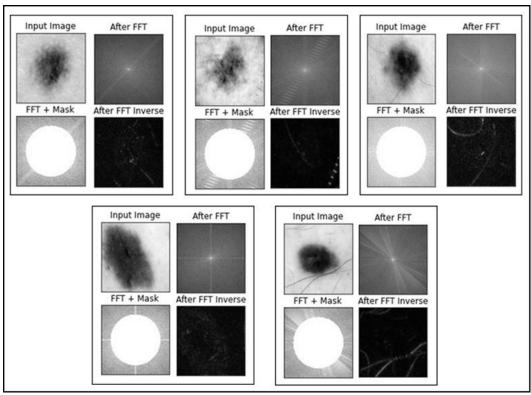
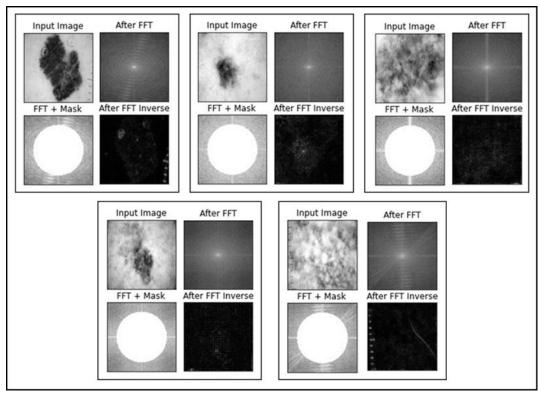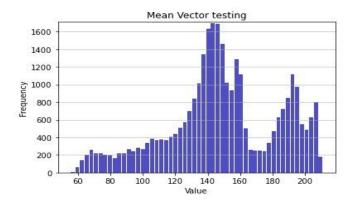**Figure. 9a.** The output of Class 1 in preprocessing stage.

Figure. 9b. The output of Class 2 in preprocessing stage.

5.2.2 The results of classification stage

In this sup unit, the consequences of the future system in classification stage for both of machine and deep learning have been presented as the following:

- *Machine learning algorithms*

The system is divided to two steps characteristic extraction the use of PCA algorithm and use the RF, and NB for classification. The first subsystem is the classification stage first subsystem is, which is built on a machine machine-learning algorithm and employs two of the most prevalent algorithms, Random Forest (RF), and Nave Bayesian (NB). The PCA algorithm is employed to extract the features at the first stage of classification as discussed above. However, the values the mean vectors for two classes of skin cancer images is shown in figure. 10.

Figure. 10. The mean vectors of skin cancer images for two classes.

Moreover, the results of applied algorithms were calculated according to the confusion matrix. Subsequently, the Naïve Bayesian achieved a satisfactory result in Skin cancer detection with accuracy of 96% tested with amount images of 660. Whereas, the Random Forest have been attained an correctness of 97% with the same amount of testing images.

- *Deep learning algorithm*

The suggested DCNN system is the second subsystem, and it is classified based on a deep learning method that employs a CNN algorithm. After dividing the dataset in to training, testing, and validation, with 200 epochs and the CNN algorithm runs for every epoch 230 times. The epoch step results are training in seconds, training accuracy, validation accuracy, validation loss, and training loss. The validation and training histograms are depicted in figure.11 a, b shown histogram of training and validation accuracy. However, based on the results, Deep CNN produced the greatest results with an accuracy of 99.5 percent when compared to the two machine learning algorithms and the associated work.
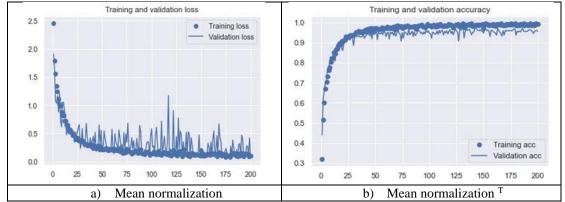

| a)   Mean normalization | b)   Mean normalization ^{T} |

Figure. 11. Histogram of training and validation Accuracy.

6. Analysis And Discussion

Skin cancer detection has long been a hot topic since it is exposed to the outside environment and is very susceptible to illness. Normally, precise and quick illness detection plays an essential role in managing skin cancer disease, because helpful protective measures are frequently undertaken following proper diagnosis. To identify and diagnose skin cancer disorders, several strategies have been proposed, developed, and deployed. The majority of these are incapable of detecting and diagnosing planets' diseases with high precision. This study suggested, implemented, assessed, and compared an autonomous method for detecting and diagnosing early skin cancer disorders. Deep Conventional Neural Network is used to power the system. However, the results demonstrated that the suggested approach is effective for detecting and diagnosing early skin cancer disorders. The majority of approaches in the literature indicate classification accuracies ranging from 50% to 90%. When additional cases of skin cancer are added, such approaches may not perform as well.

Furthermore, as discussed in the preceding chapters, two aspects had been proposed first one is improving detection and accuracy by enhanced DCNN, second one is machine learning technique and its implementation, testing, evaluation and design to detect and diagnose skin cancer. These are the Naive Bayes and Random Forest algorithms. Furthermore, the ISIS dataset was utilized to test and assess the performance of both subsystems, with 70% of the data being usage for exercise and 30% for testing.

Following that, it is seen that the DCNN acquired the highest results when compared to the other feature of machine learning and the frequent work of Daghrir et al. (Daghrir et al., 2020), Kumar1 et al. (Kumar et al., 2020), and Boman and Volminger (Boman & Volminger, 2018). Table (2) compares the outcomes of DCNN with machine learning (Random Forest, and Naive Bayes) and related work.

Table 2. Proposed Model Results Comparison with Past Literature Work

Model	Techniques	Dataset	Accuracy%
Daghrir et al.	CNN	ISIC	88.4%
Kumar1 et al.	ANN	HAM10000	97.4%
Boman and Volminger,	CNN	ISIC	91%
Machin learning	NB	ISIS	96%
	RF	ISIS	97%
Our proposed system	**DCNN**	**ISIS**	**99.5%**

7. Conclusion

Nowadays, detecting and diagnosing skin cancer disorders at an early degree is a challenging chore that women may face. Furthermore, technology performs a crucial position in the identification and diagnosis of skin cancer. In this work, the greatest common of Deep and machine learning algorithms have been employed for an early and accurate skin cancer diagnosis. Furthermore, based on the findings obtained, it is seen that the proposed system delivered the best outcomes when compared to the related work. Using the ISIS dataset, the proposed system was analyzed and tested. The suggested system can be used at a hospital, a health care facility, or anywhere else required. For future work, it is optional to test the proposed system with different dataset and different deep learning algorithms.

Reference

Boman, J., & Volminger, A. (2018). Evaluating a deep convolutional neural network for classification of skin cancer. In.

Bray, F., Ferlay, J., Soerjomataram, I., Siegel, R. L., Torre, L. A., & Jemal, A. (2018). Global cancer statistics 2018: GLOBOCAN estimates of incidence and mortality worldwide for 36 cancers in 185 countries. *CA: a cancer journal for clinicians, 68*(6), 394-424 .

Brekhna, B., Mahmood, A., Zhou, Y., & Zhang, C. (2017). Robustness analysis of superpixel algorithms to image blur, additive Gaussian noise, and impulse noise. *Journal of Electronic Imaging, 26*(6), 061604 .

Daghrir, J., Tlig, L., Bouchouicha, M., & Sayadi, M. (2020). *Melanoma skin cancer detection using deep learning and classical machine learning techniques: A hybrid approach* .Paper presented at the 2020 5th international conference on advanced technologies for signal and image processing (ATSIP).

Dorj, U.-O., Lee, K.-K., Choi, J.-Y., & Lee, M. (2018). The skin cancer classification using deep convolutional neural network. *Multimedia Tools and Applications, 77*(8), 9909-9924 .

Gedraite, E. S., & Hadad, M. (2011). *Investigation on the effect of a Gaussian Blur in image filtering and segmentation.* Paper presented at the Proceedings ELMAR-2011.

Grigoryan, A. M., & Agaian, S. S. (2 .(020New look on quantum representation of images: Fourier transform representation. *Quantum Information Processing, 19*(5), 1-26 .

Kadampur, M. A., & Al Riyaee, S. (2020). Skin cancer detection: Applying a deep learning based model driven architecture in the cloud for classifying dermal cell images. *Informatics in Medicine Unlocked, 18*, 100282 .

Krive, J., Patel, M., Gehm, L., Mackey, M., Kulstad, E., Lussier, Y. A., & Boyd, A. D. (2015). The complexity and challenges of the international classification of diseases, ninth revision, clinical modification to international classification of diseases, 10th revision, clinical modification transition in eds. *The American journal of emergency medicine, 33*(5), 713-718 .

Ku, J., Harakeh, A., & Waslander, S. L. (2 .(018*In defense of classical image processing: Fast depth completion on the cpu.* Paper presented at the 2018 15th Conference on Computer and Robot Vision (CRV.(

Kumar, M., Alshehri, M., AlGhamdi, R., Sharma, P., & Deep, V. (2020). A de-ann inspired skin cancer detection approach using fuzzy c-means clustering. *Mobile Networks and Applications, 25*(4), 1319-1329 .

Lewis, D. D. (1998). *Naive (Bayes) at forty: The independence assumption in information retrieval.* Paper presented at the European conference on machine learning.

Mahesh, B. (2020). Machine learning algorithms-a review. *International Journal of Science and Research (IJSR).[Internet], 9*, 381-386 .

Munir, K., Elahi, H., Ayub, A., Frezza, F., & Rizzi, A. (2019). Cancer diagnosis using deep learning :a bibliographic review. *Cancers, 11*(9), 1235 .

Nahata, H., & Singh, S. P. (2020). Deep learning solutions for skin cancer detection and diagnosis. In *Machine Learning with Health Care Perspective* (pp. 159-182): Springer.

Pacheco, A. G., Ali, A.-R., & Trappenberg, T. (2019). Skin cancer detection based on deep learning and entropy to detect outlier samples. *arXiv preprint arXiv:1909.04525* .

Pranckevičius, T., & Marcinkevičius, V. (2017). Comparison of naive bayes, random forest, decision tree, support vector machines, and logistic regression classifiers for text reviews classification. *Baltic Journal of Modern Computing, 5*(2), 221 .

Rey-Barroso, L., Peña-Gutiérrez, S., Yáñez, C., Burgos-Fernández, F. J., Vilaseca, M., & Royo, S. (2021). Optical Technologies for the Improvement of Skin Cancer Diagnosis: A Review. *Sensors, 21*(1), 252 .

Salvi, M., Acharya, U. R., Molinari, F., & Meiburger, K. M. (2021). The impact of pre-and post-image processing techniques on deep learning frameworks: A comprehensive review for digital pathology image analysis. *Computers in Biology and Medicine, 128*, 104129 .

Speiser, J. L., Miller, M. E., Tooze, J., & Ip, E. (2019). A comparison of random forest variable selection methods for classification prediction modeling. *Expert systems with applications, 134*, 93-101 .

Wang, A., Zhang, W., & Wei, X. (2019). A review on weed detection using ground-based machine vision and image processing techniques. *Computers and electronics in agriculture, 158*, 226-240 .

Yang, Y.-G., Zou, L., Zhou ,Y.-H., & Shi, W.-M. (2020). Visually meaningful encryption for color images by using Qi hyper-chaotic system and singular value decomposition in YCbCr color space. *Optik, 213*, 164422 .

Zhang, L., Gao, H. J., Zhang, J., & Badami, B. (2019). Optimization of the convolutional neural networks for automatic detection of skin cancer. *Open Medicine, 15*(1), 27-37 .

Zhang, N., Cai, Y.-X., Wang, Y.-Y., Tian, Y.-T., Wang, X.-L., & Badami, B. (2020). Skin cancer diagnosis based on optimized convolutional neural network. *Artificial intelligence in medicine, 102*, 101756 .